



## Performance Comparison between FIT and MoM Based Solvers for Microstrip Patch Array Antennas with Conventional Geometries

Ouadiaa BARROU<sup>1</sup>, Abdelkebir EL AMRI<sup>2</sup>, Abdelati REHA<sup>3</sup> and Nirmine HAMMOUCH<sup>4</sup>

<sup>1,2</sup> DRITM Laboratory, CED Engineering Sciences, ESTC, Hassan II University of Casablanca, Casablanca, Morocco

<sup>3</sup> Electronic Department, ISGA Marrakech, Marrakech, Morocco

<sup>4</sup> Smart Communications Research Team, E3S Research Center, EMI, Mohammed V University, Rabat, Morocco

<sup>1</sup>ouadiaa.barrou@gmail.com, <sup>2</sup>elamri\_abdelkebir@yahoo.fr, <sup>3</sup>abdelati.reha@isga.ma, <sup>4</sup>hammouchnirmine1@gmail.com

### ABSTRACT

In this paper, a comparative study of Microstrip patch array antennas based on conventional geometries was performed. First, single element patch antennas with rectangular, triangular and circular geometry were studied based on the Transmission Line Model (TLM). The results have been optimized and validated by FEKO a solver which is based on the Method Of the Moments (MoM) after that it validate by CST a solver which is based on the Finite Integration Technique (FIT). Thereafter, we compare the performances of the antennas versus the geometry shape. Next, two and four elements for each geometry are studied in order to analyze their effect on the HPBW (Half Power Beam Width) and the total gain. A comparison of the results given by FEKO and CST is performed.

**Keywords:** Array, antennas, Beamforming, circular, Finite Integration Technique, Hexagonal, Method Of Moments, rectangular, triangular.

### 1. INTRODUCTION

Nowadays, the explosion of wireless telecommunication systems to performance requirements continues to grow, particularly in aeronautical, military and governmental applications where low weight, low cost, high performance, multi-band and Ultra Wide Band behavior are a necessity which implies low profile antennas. The patch antennas, which are the subject of several researches, are based on dielectric substrates and combine small size, small overcrowding, ease of manufacturing and even networking [1]–[7].

Grouping radiating patch elements improves performances in particular: Gain and Directivity, also, the HPBW be-comes narrow. It's allows other functions such

as: controlling the direction of the radiating pattern and beam forming.

The array antenna is composed of N radiating elements placed on specific positions. The feeding is also done in a specific manner to achieve one of the objectives: a high gain or to steer the radiating pattern or to have a beam forming [1], [2], [8]–[10].

The objective of this work is the performance comparison between FIT (*Finite Integration Technique*) and MoM (Method Of Moments) based solvers for microstrip patch array antennas with conventional geometries such as: rectangle, triangle and circle.

In the first section, single element patch antennas are studies, in the following sections, for each geometry, two and four elements patch array antennas are studied.

### 2. Antennas Modeling Techniques and Numerical Methods for Maxwell's Equations

Several methods are used for antenna analysis. The most important are:

- Transmission Line Model [1], [10], [11].
- Resonant Cavity Model [10], [11]
- Numerical methods for solving Maxwell's

equations. Several techniques are adopted, the most popular are: the Method of Moments (MoM), the Finite Elements Method (FEM), Finite Integration Technique (FIT) and Finite Difference Time Domain (FDTD) [11], [10], [8], [12]–[16].

The method of the transmission lines is the simplest; it gives good physical interpretations but hardly models the coupling. The resonant cavity method is more accurate

than the transmission line method but it is more complex. Numerical methods are more accurate than the last two methods because they solve Maxwell's equations very precisely, even for complex structures. Several solvers are used in the industrial world as well as in the research laboratories, for example: FEKO which is mainly based on the Method Of Moments (MoM) in addition to some additional methods such as Finite Element Method (FEM), Finite Difference Time Domain (FDTD) and others [17], CST Microwave Studio which is based principally on Finite Integration Technique (FIT) and HFSS methods which is based on Finite Elements Method (FEM)[15], [16].

In the next section, a study of some microstrip patch antennas will be done using two different solvers; the first one is FEKO based on the MoM, the second one is CST based on the FIT.

### 3. SINGLE ELEMENTS DESIGN STUDY

A microstrip radiating element can be used alone or even networking, whatever the case the overall goal of a design is to achieve a stipulated operating performance like in terms of directivity and gain at a specific frequency for this reason the first decision is to select a suitable antenna dimensions.

Our antennas design is made on a FR4 substrate with relative permittivity  $\epsilon_r=4.4$  and height of the dielectric substrate  $h=1.6\text{mm}$ . To design patch antenna array of  $2 \times 1$  and  $4 \times 1$ , we follow the following steps:

#### 3.1 Microstrip Rectangular patch antenna geometry

The dimensions of a rectangular patch antenna are calculated initially based on the theory of transmission lines summarized in figure 1[10], [11].

Using the previous algorithm and after optimization with FEKO, the dimensions of the patch antenna with a resonant frequency of 2.45GHz are:

The width:  $W_p= 35.52\text{mm}$

The length:  $L_p= 27.45\text{mm}$ .

The width of the microstrip feeding line should be  $W_f= 2.56 \text{ mm}$  according to the equation (1) [10], [11].

$$Z_0 = \frac{120\pi}{\sqrt{\epsilon_r} \left( \frac{W_f}{h} + 1.393 + 0.667 \ln \left( \frac{W_f}{h} + 1.44 \right) \right)} \quad (1)$$

With:

$Z_0$ : the characteristic impedance of the microstrip line.

$W_f$ : the width of the microstrip line.

$h$ : the high of the substrate.

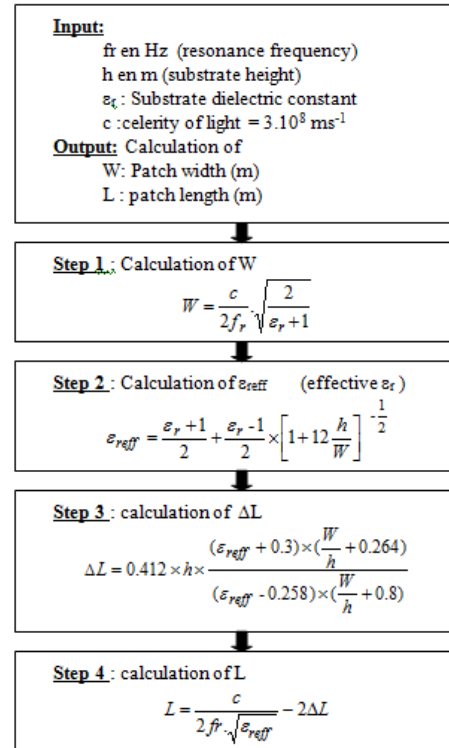


Fig. 1. Algorithm design of a rectangular patch antenna (Method of transmission lines)

To have a good impedance matching, the other parameters should be:  $Y_0=7.5\text{mm}$  (figure2).

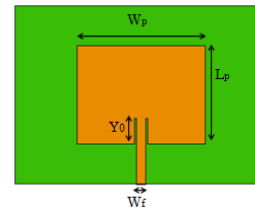


Fig. 2. Microstrip rectangular patch antenna

Figure 3(a) shows the  $S_{11}$  parameter versus frequencies and figure 3(b) shows the 3D total gain with FEKO, we observe that the maximum gain is 5dB.

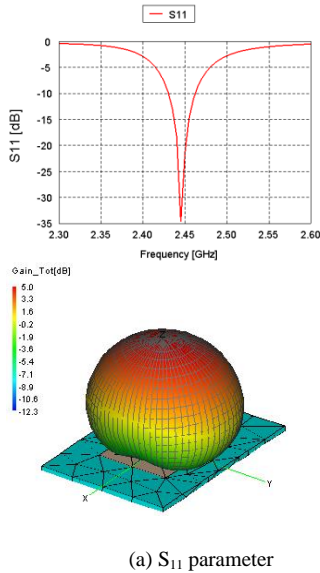


Fig. 3.  $S_{11}$  parameter and 3D-Total gain for the microstrip rectangular patch Antenna with FEKO

The results have been validated by CST a FIT based solver (figure 4 and 5).

We notice that the two resonance frequencies are respectively 2.45GHz (FEKO) and 2.54GHz (CST). The two maximum gains are respectively 5dB (FEKO) and 4.83dB (CST). We consider that the results are almost similar.

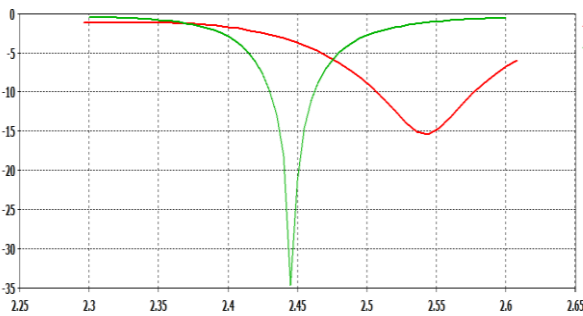


Fig. 4. Comparison  $S_{11}$  parameter between CST and CADFEKO

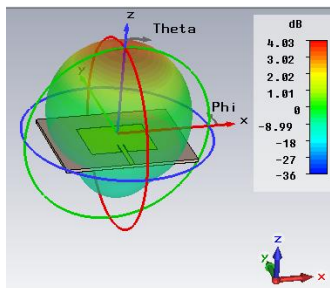


Fig. 5. Total gain for the microstrip rectangular patch Antenna

### 3.2 Microstrip triangular patch antenna geometry

Equation (2) and (3) shows the fundamental mode resonant frequency of equilateral triangular patch antenna

$$f_r = \frac{2c}{3a_e \sqrt{\epsilon_r}} \quad (2)$$

$$\text{And } a_e = a + \frac{h}{\sqrt{\epsilon_r}} \quad (3)$$

With:

c: Speed of light

a: Patch side length (figure 6)

$a_e$ : the effective patch side length

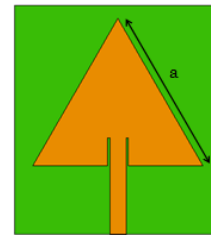
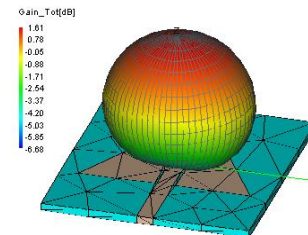
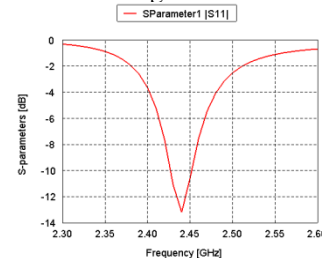


Fig. 6. Microstrip triangular patch antenna

By applying the previous equations and after optimization with FEKO, the side length of the triangular patch antenna with a resonant frequency of 2.45GHz is  $a = 37.07\text{mm}$ . Figure 7(a) shows the  $S_{11}$  parameter versus frequencies and figure 7(b) shows the 3D total gain, we observe that the maximum gain is 1.6dB.



(a)  $S_{11}$  parameter (b) 3D-Total gain

Fig. 7.  $S_{11}$  parameter and 3D-Total gain for the microstrip triangular patch antenna

The results have been validated by CST (Figure 8 and 9).

We notice that the two resonance frequencies are respectively 2.44GHz (FEKO) and 2.51GHz (CST). The two maximum gains are respectively 1.61dB (FEKO) and 2.16dB (CST). We consider that the results are almost similar.

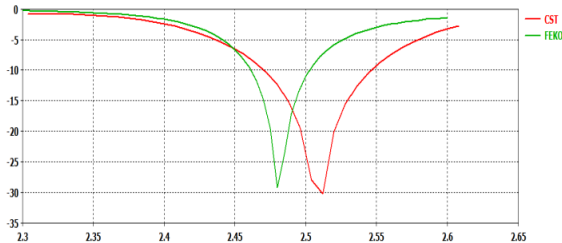


Fig. 8.  $S_{11}$  parameter

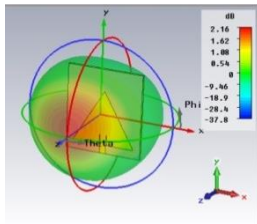


Fig. 9. 3D-Total gain for the microstrip triangular patch antenna

### 3.3 Microstrip circular patch antenna geometry

According to Balanis[11], the fundamental resonance frequency of a circular patch antenna is given by the equation (4)

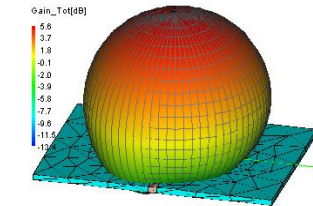
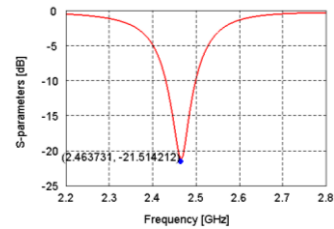
$$f_r = \frac{C.X_{mn}}{2.\pi.a_e.\sqrt{\epsilon_r}} \quad (4)$$

Where  $f_r$  is the resonant frequency of the patch,  $X_{mn} = 1.8412$  for the dominant mode  $TM_{11}$ ,  $C$  is the velocity of light in free space,  $\epsilon_r$  is the relative permittivity of the substrate and  $a_e$  is the effective radius of the circular patch and which given by the equation (5).

$$a_e = a \left[ 1 + \frac{2h}{a\pi\epsilon_r} \left( \ln\left(\frac{\pi a}{2h}\right) + 1.7726 \right) \right]^{1/2} \quad (5)$$

Where  $a$  is the radius of the circular patch and  $h$  is the height of the substrate.

By applying the previous equations and after optimization with FEKO, the radius of the circular patch antenna with a resonant frequency of 2.45GHz is  $a = 16.82\text{mm}$ . Figure 10(a) shows the  $S_{11}$  parameter versus frequencies and figure 10(b) shows the 3D total gain, we observe that the maximum gain is 5.6dB.



(a)  $S_{11}$  parameter (b) 3D-Total gain

Fig. 10.  $S_{11}$  parameter and 3D-Total gain for the microstrip circular patch antenna

The results have been validated by CST (Figure 8 and 9).

We notice that the two resonance frequencies are respectively 2.45GHz (FEKO) and 2.45GHz (CST). The two maximum gains are respectively 5.6dB (FEKO) and 3.46dB (CST). We consider that the results are almost similar.

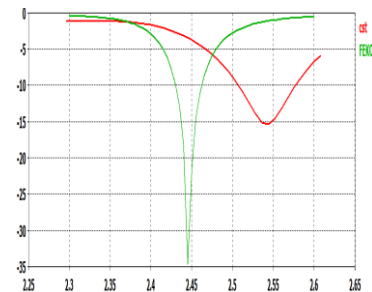


Fig. 11.  $S_{11}$  parameter for microstrip circular patch antenna

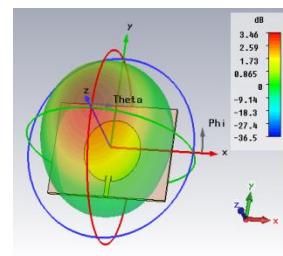


Fig. 12. the 3D-Total gain for the microstrip circular patch antenna

To summarize this first section, we observe that the circular configuration is the better solution to design patch antenna with an important gain. Also, we remark that the two solvers that are based on different numerical methods give almost similar results.

Table 1: comparison between the results obtained by FEKO (MoM) and CST (FIT)

Configuration	Resonance frequency (GHz)		Maximum Gain (dB)	
	FEKO	CST	FEKO	CST
Rectangular	2.45	2.54	5	4.83
Triangular	2.44	2.51	1.61	2.16
Circular	2.45	2.45	5.6	3.46

In the next sections, the array patch antennas having the same previous geometries will be studied using the same solvers. To make fair comparison, we use the same substrate used in single element ( $\epsilon_r= 4.4$  and thickness  $h=1.6$  mm).

#### 4. RECTANGULAR PATCH ARRAY STUDY

The radiating elements are fed by microstrip lines having the same width ( $w_f=3$ mm), inset feed are placed to ensure a good impedance matching. The spacing between elements is optimized with FEKO to have a good efficiency and to have a low SLL (Side Lobe Level) ( $d=0.65\lambda$ ) (Fig 13). Figure 14 shows the comparison of E-plane radiation pattern for the single, two and four radiation elements. We observe that more the element number increases, the maximum gain increases and the HPBW (Half Power Beam Width) decreases. Those results are summarized in table 2.

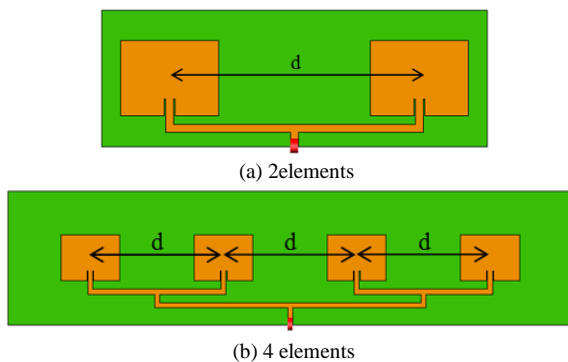


Fig. 13. Rectangular array antennas

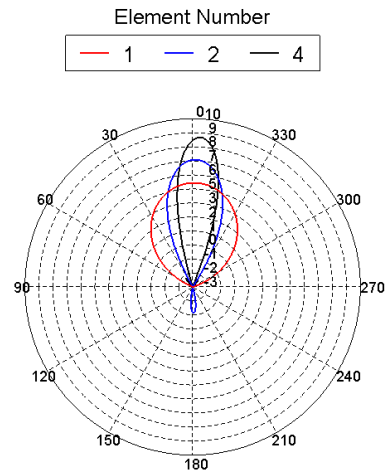


Fig. 14. The comparison of E-plane radiation pattern for the single, two and four radiation elements.

Table 2: Gains and HPBW versus element number (FEKO)

Element number	Maximum Gain (dB)	HPBW
1	5	84°
2	6.82	40°
4	8.35	28°

The results have been validated by CST (Table 3). We notice that the results are almost similar even if we remark some small differences.

Table 3: Gains and HPBW versus element number (CST)

Element number	Maximum Gain (dB)	HPBW
1	4.03	80°
2	6.98	34°
4	7.8	16°

### 5. TRIANGULAR PATCH ARRAY STUDY

The radiating elements are fed by microstrip lines having the same width ( $w_f=3\text{mm}$ ), inset feed are placed to ensure a good impedance matching. The spacing between elements is optimized with FEKO to have a good efficiency and to have a low SLL (Side Lobe Level) ( $d=0.76\lambda$ ) (Fig 15). Figure 16 shows the comparison of E-plane radiation pattern for the single, two and four radiation elements. We observe that more the element number increases, the maximum gain increases and the HPBW (Half Power Beam Width) decreases. Those results are summarized in table 4.

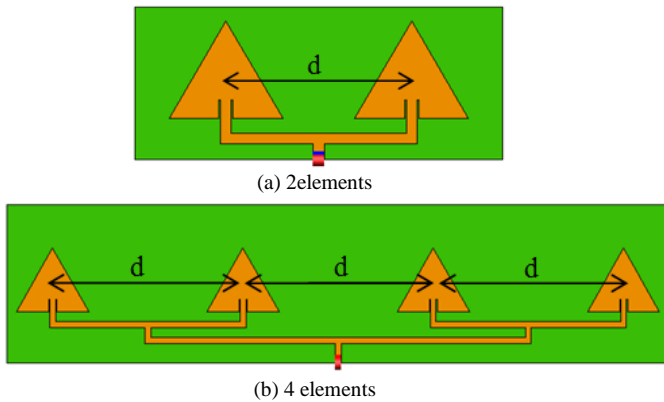


Fig. 15. Triangular array antennas

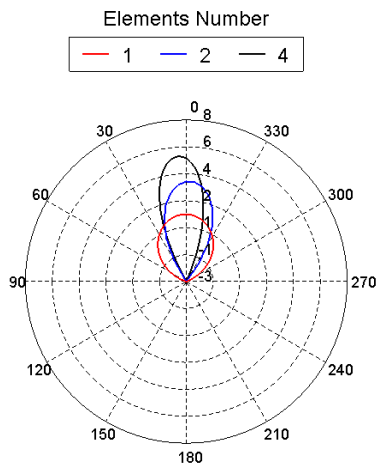


Fig. 16. The comparison of E-plane radiation pattern for the single, two and four radiation elements.

Table 4: Gains and HPBW versus element number (FEKO)

Element number	Maximum Gain (dB)	HPBW
1	1.6	108°
2	3.8	56°
4	5.53	24°

The results have been validated by CST (Table 5). We notice that the results are almost similar even if we remark some small differences.

Table 5: Gains and HPBW versus element number (CST)

Element number	Maximum Gain (dB)	HPBW
1	2.16	97.7°
2	4.04	52°
4	6.15	23.2°

### 6. CIRCULAR PATCH ARRAY STUDY

The radiating elements are fed by microstrip lines having the same width ( $w_f=3\text{mm}$ ), inset feed are placed to ensure a good impedance matching. The spacing between elements is optimized with FEKO to have a good efficiency and to have a low SLL (Side Lobe Level) ( $d=0.5\lambda$ ) (Fig 17). Figure 18 shows the comparison of E-plane radiation pattern for the single, two and four radiation elements. We observe that more the element number increases, the maximum gain increases and the HPBW (Half Power Beam Width) decreases. Those results are summarized in table 6.

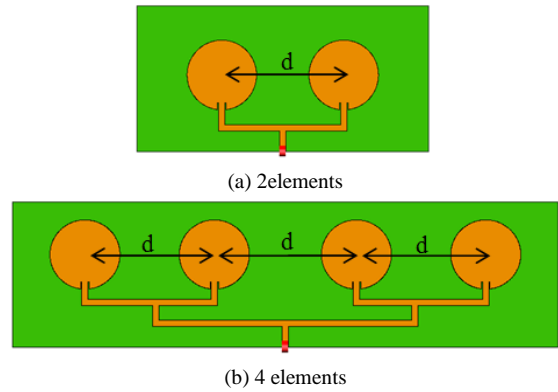
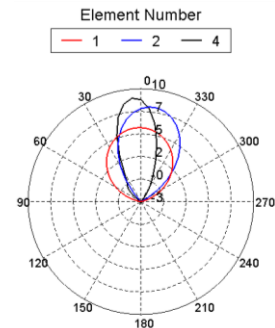


Fig. 17. Circular array antennas



The results have been validated by CST (Table 7). We notice that the results are almost similar even if we remark some small differences.

Fig. 18. The comparison of E-plane radiation pattern for the single, two and four radiation elements.

Table 6: Gains and HPBW versus element number (FEKO)

Element number	Maximum Gain (dB)	HPBW
1	5.6	70°
2	7.95	55°
4	8.96	30°

Table 7: Gains and HPBW versus element number (CST)

Element number	Maximum Gain (dB)	HPBW
1	3.46	98°
2	6.09	60°
4	8	36°

## 7. CONCLUSIONS

In this paper, several designs of micorstrip arrays antennas such as rectangular, triangular and circular patch antennas array are studied. Specifically, 4x1, 2x1, and single element of both shapes are designed and simulated by FEKO based on the Method Of Moments (MoM) and CST based on the Finite Integration Technique (FIT). In the first time, a comparison between the different shapes was carried out for one radiating element, at this level we can conclude that the circular configuration is the better solution to design patch antenna with an important gain. In the next steps, for all the shapes of the radiating elements, the increase of the radiating elements number induced the increase of the gain and the decrease of HPBW. We observe that the circular array patch antenna presents the bigger total gain and the rectangular array patch antenna presents the lower HPBW. In the next studies, we hope validate these results by manufacturing and real measurements.

## REFERENCES

[1] O. Barrou, A. E. Amri, A. Reha, et M. Tarbouch, « Microstrip patch array antennas based on conventional geometries », in 2017 International Conference on Electrical and Information Technologies (ICEIT), Rabat, 2017, p. 1-6.

[2] O. BARROU, A. EL AMRI, et A. REHA, « Study of electronically beam scanning of linear array antennas », présenté à International Conference On Computing Wireless & Communication Systems (ICCWCS'16), FST, SETTAT, nov-2016.

[3] A. A. Ibrahim, M. A. Abdalla, et A. Boutejdar, « A PRINTED COMPACT BAND-NOTCHED ANTENNA USING OCTAGONAL RADIATING PATCH AND MEANDER SLOT TECHNIQUE FOR UWB APPLICATIONS », Prog. Electromagn. Res. M, vol. 54, p. 153-162, 2017.

[4] A. A. Ibrahim, M. A. Abdalla, et A. Boutejdar, « Resonator switching techniques for notched ultra-wideband antenna in wireless applications », IET

Microw. Antennas Propag., vol. 9, no 13, p. 1468-1477, oct. 2015.

[5] S. Chandran, « Smart Antennas for Wireless Communications (with MATLAB) (Gross, F.; 2005) [Reviews and Abstracts », IEEE Antennas Propag. Mag., vol. 51, no 3, p. 134-134, juin 2009.

[6] A. Boutejdar, A. A. Ibrahim, et E. P. Burte, « A Compact Multiple Band-Notched Planer Antenna with Enhanced Bandwidth Using Parasitic Strip Lumped Capacitors and DGS-Technique », TELKOMNIKA Indones. J. Electr. Eng., vol. 13, no 2, févr. 2015.

[7] A. Boutejdar et W. Abd Ellatif, « A novel compact UWB monopole antenna with enhanced bandwidth using triangular defected microstrip structure and stepped cut technique », Microw. Opt. Technol. Lett., vol. 58, no 6, p. 1514-1519, juin 2016.

[8] T. A. Milligan, Modern antenna design, 2nd ed. Hoboken, N.J: IEEE Press : Wiley-Interscience, 2005.

[9] R. L. Haupt, Antenna arrays: a computational approach. Hoboken, N.J: Wiley-IEEE Press, 2010.

[10] R. S. Elliott, Antenna theory and design, Revised ed. Hoboken, N.J: John Wiley & Sons, 2003.

[11] C. A. Balanis, Antenna theory: analysis and design, 3rd ed. Hoboken, NJ: John Wiley, 2005.

[12] W. C. Gibson, The Method of moments in electromagnetics, Second edition. Boca Raton: CRC Press/Taylor & Francis, 2014.

[13] J.-M. Jin, The finite element method in electromagnetics, 2nd ed. New York: John Wiley & Sons, 2002.

[14] J.-M. Jin et D. J. Riley, Finite element analysis of antennas and arrays. Hoboken, N.J: John Wiley & Sons : IEEE Press, 2009.

[15] A. Reha et A. O. Said, « Tri-Band Fractal Antennas for RFID Applications », Wirel. Eng. Technol., vol. 04, no 04, p. 171-176, 2013.

[16] A. REHA, A. EL AMRI, O. Benhammouch, et A. Oulad Said, « Dual-band antenna for 2.45/5.8 GHz RFID applications », présenté à International Conference On Multimedia Computing and Systems ICMCS 14, Marrakech, avr-2014.

[17] A. Z. Elsherbeni, P. Nayeri, et C. J. Reddy, Antenna analysis and design using FEKO electromagnetic simulation software. Edison, NJ: SciTech Publishing, an imprint of the IET, 2014.